water

MDPI

Article

Risk Assessment of Nonpoint Source Pollution in the Huaihe River Basin

Huiling Zhao, Jiaxiao Zheng, Yuke Zhu, Luyi Li and Xitian Cai *

School of Civil Engineering, Sun Yat-sen University, Guangzhou 510275, China
* Correspondence: caixitian@mail.sysu.edu.cn

Abstract: After years of treatment, the water pollution situation in the Huaihe River Basin (HRB) is still grim, and agricultural nonpoint source pollution has become the leading cause of the problem. However, agricultural nonpoint source pollution in the HRB is complicated due to the compounding effects of multiple factors. In this study, we first applied the export coefficient model to estimate the total nitrogen (TN) and total phosphorus (TP) loads used as two pollution source indicators in HRB. Then we constructed an index evaluation system of nonpoint source pollution risk by coupling the two source indicators with five additional indicators: rainfall erosion, river network distribution, soil erodibility, slope length, and land use. The primary source of TN and TP loads is fertilizer application (81.96%), followed by livestock and poultry breeding (16.3%) and rural domestic wastes (1.74%). The risk assessment results indicate that 66.43% of the HRB is at medium to high risk of nonpoint source pollution, 12.37% is at high risk, and 11.20% is at low risk. Moreover, the medium-to-high-risk areas are mainly concentrated in the Henan and Anhui provinces. In contrast, the medium-risk regions are mainly distributed along the mainstream of the Huaihe River. Finally, the observed water quality categories were used to verify our findings. The controlling areas of nonpoint source pollution in HRB are identified. This study could provide a scientific basis for effectively preventing and treating water pollution in the HRB.

Keywords: nonpoint source pollution; risk assessment; Huaihe River Basin

check for updates

Citation: Zhao, H.; Zheng, J.; Zhu, Y.; Li, L.; Cai, X. Risk Assessment of Nonpoint Source Pollution in the Huaihe River Basin. *Water* **2022**, *14*, 3505. https://doi.org/10.3390/w14213505

Academic Editors: Lei Chen, Hui Xie, Lei Wu and Liang Zhang

Received: 30 September 2022
Accepted: 27 October 2022
Published: 2 November 2022

1. Introduction

Water is an important strategic resource essential for humans and the ecosystem. It provides drinking, sanitation, and hygiene services for human beings and is an indispensable input in the agriculture, energy, and industry sectors. Also, water has an important ecological role, such as maintaining base flow to ensure biodiversity. However, global water demand has been increasing, and water scarcity has become a severe problem worldwide [1,2]. Apart from climate change [3,4] and population growth, water quality deterioration is an important cause of water scarcity [5,6]. Water quality is affected by multiple factors (e.g., land use and vegetation) and shows spatial-temporal variation [7]. Usually, the water quality of wet regions has higher seasonal variation than that of dry regions [8], and the water quality of cold climatic regions has a smaller longitudinal variation than that of other regions [9]. Therefore, water pollution not only causes water resource crises but also causes damage to the aquatic ecosystem.

Depending on the sources, water pollution is often classified into two main categories: point source and nonpoint source pollution. The point source pollutants [10], released from a fixed location, can be controlled relatively well by compulsory measures such as improving the wastewater discharge standards or shutting down factories. On the contrary, nonpoint source pollution is difficult to monitor and control because of its widespread in space, the wide variety of pollutants, no fixed or concentrated discharge points, and the randomness and intermittency due to rainfall-runoff, the carrier of migration and transformation [11]. Moreover, in recent years, due to rapid urbanization, the expansion of livestock and poultry breeding, and the application of pesticides and chemical fertilizers [12,13] in the planting industry, the total nitrogen and phosphorus loads have increased significantly [14–17]. As a result, nonpoint source pollution is becoming an important cause of surface water pollution in China [18].

Currently, the methods for nonpoint source pollution estimation mainly include (a) the use of physical-based models to simulate the migration and transformation of pollutants to analyze the water quality quantitatively [19], (b) the use of the export coefficient model (ECM) to estimate the pollutants loads and analyze the contributions of different pollution sources, and (c) the establishment of index evaluation system by comprehensively considering multiple factors (e.g., climate, hydrology, and geology) to identify the potential risk controlling area of nonpoint source pollution. Physical-based models such as the Soil and Water Assessment Tool (SWAT) [20,21], the Annualized Agricultural Non-Point Source Pollution Model (AnnAGNPS) [22,23], and the Hydrologic Simulation Program-Fortran model (HSPF) [24,25], require a large amount of input data (e.g., atmospheric forcing, soil, land use and land cover, and fertilizer applications), which is usually difficult to obtain [26]. Furthermore, these models usually consist of hydrological processes, soil erosion, and nutrient transportation modules. Therefore, numerous parameters need to be determined by model calibration [27]. Moreover, the application of a model developed for a location to a new location needs to be adjusted based on the topographic and geological differences, which is relatively complex. Due to limited data and complex mechanisms, it is challenging to use physical-based models.

The ECM, proposed by Omernik [28], was first used to predict nutrient load. The ECM predicted the nitrogen and phosphorus loss from individual sources within the catchment, applying different export coefficients for different sources [28,29]. The original ECM did not consider the influence of meteorological factors and underlying variation on the transportation of nutrients. The ECM has been improved by coupling the nutrient transportation process and considering meteorological factors. For example, precipitation and terrain factors were introduced to characterize spatial heterogeneity [30,31]. Compared with physical-based models, the data required by ECM is readily available. Many studies have applied this method to estimate nitrogen and phosphorus loads [32,33]. The index system method selects the factors that potentially impact NPS and assigns each factor weight to rank NPS risk areas. Frequently used index system methods include Agricultural Non-point Pollution Potential Index (APPI) and the Phosphorus Index (PI). The APPI system was constructed by H.Y. Guo [34,35] to identify the critical areas of NPS in the Taihu Lake region. The PI method was developed by J.L. Lemunyon [36] to assess the vulnerability of phosphorus movement. The index system method is technically simple and has a low requirement in computational cost. Therefore, it can quickly identify the hotspots of nonpoint source pollution.

The Huaihe River is one of the seven major rivers in China, and its water pollution began in the 1970s. After years of treatment, the water quality of the Huaihe River has been significantly improved. Still, there is a certain gap with other major rivers, such as the Pearl River and the Yangtze River [37]. The field report by Li [38] on the Huaihe River Basin (HRB) shows that the failure to eradicate agricultural nonpoint source pollution is still one of the most important factors in the unsatisfactory water quality of the Huaihe River. Existing risk assessment systems of nonpoint source pollution in the HRB either only predict pollutant loads (e.g., nitrogen and phosphorus) from the perspective of pollution sources or only consider the promotion/inhibition factors (e.g., hydrological, climate, topographic, and geological factors) on pollutants entering the water bodies from the migration process. For example, Song [39] used the ECM to calculate the total nitrogen load and emission intensity in different cities; Zhang and Huang [40] considered the hydrogeological indexes, such as rainfall and soil, to determine the regions with the highest potential nitrogen loss.

In this study, we first applied the ECM to estimate the TN and TP loads used as two pollution source indicators in HRB. Then we constructed an index evaluation system of nonpoint source pollution risk by coupling the two source indicators with hydrological and climate indicators and topographic and geological indicators. It is expected to quickly identify the high-risk areas of nonpoint source pollution and provide a basis for targeted and efficient prevention and control of nonpoint source pollution.

2. Materials and Methods

2.1. Study Area

The Huaihe River, with a total length of about 1000 km, originates from the northern of Tongbai Mountain, passing east through Henan and Anhui and flowing into the Yellow Sea in Jiangsu Province. The HRB (111°55′–121°45′ E, 30°55′–36°36′ N) is between the Yangtze River and the Yellow River. The basin area is up to 269,600 km^2, and the annual average water resource is about 79.4 billion m^3. Located in the semi-humid monsoon climate zone, the mean annual precipitation of the HRB is about 875 mm, and the mean annual temperature is about 11~16 °C. With rain and heat over the same period, it is dry in winter and spring, while hot and rainy in summer.

With a dense population, fertile land, rich resources, and convenient transportation, HRB has become China's important grain production base [41]. It spans over 40 cities and 240 counties in Hubei, Henan, Anhui, and Shandong provinces, with a total population of 191 million. The total area of cultivated land in the basin is about 133,000 km^2, accounting for about 12% of the cultivated land area in China. However, because of the uneven distribution of precipitation temporally and spatially, flat slope, poor self-purification ability of the water body, and the population pressure, the nonpoint source pollution in the HRB is serious [37]. Meanwhile, the vast cultivated land area and developed aquaculture in the basin have become an important source of agricultural nonpoint source pollution.

In this study, to facilitate the statistics of pollution source factors, following Song, Zuo [39], the counties with less than half the area in the HRB were not included (Figure 1).

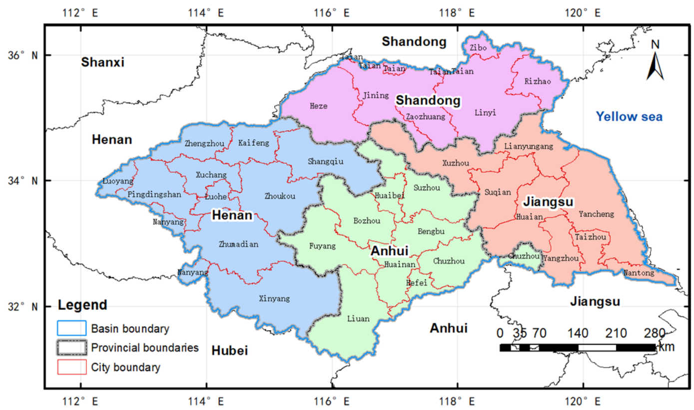

Figure 1. The Huaihe River Basin.

2.2. Calculation Methods for Each Risk Factor

2.2.1. Total Nitrogen and Total Phosphorus

In this study, the total nitrogen and total phosphorus factors were obtained by calculating the nitrogen and phosphorus loads per unit area of cultivated land in 35 cities in the HRB in 2018. In addition, we considered three major nonpoint pollution sources: rural domestic wastes, chemical fertilizer application, and livestock breeding.

(a) Rural domestic wastes were estimated by the ECM, and the export coefficient of various pollutants is multiplied by the number of people in the region to produce nitrogen and phosphorus. The export coefficient of 35 cities in the region was acquired by querying the second national pollution source census manual.

(b) The amount of fertilizer application is calculated as follows [42]:

$$\mathrm{TN} = (\mathrm{N_{fert}} + \mathrm{CF} \times 0.3 + \mathrm{P_{fert}} \times 0.185) \quad (1)$$

$$\mathrm{TP} = (\mathrm{P_{fert}} + \mathrm{CF} \times 0.3) \times 0.436 \quad (2)$$

where TN is the amount of nitrogen generated by fertilizer application; TP is the amount of phosphorus generated by fertilizer application; N_{fert} is the amount of nitrogen fertilizer application; P_{fert} is the amount of phosphorus fertilizer application; CF is the amount of compound fertilizer application.

(c) The amount of pollutants generated in livestock and poultry breeding is calculated as follows:

$$W = \sum_{i=1}^{m} P_i R_i \quad (3)$$

where W is the emission of pollutants produced by livestock and poultry breeding (kg); P_i is the number of raised livestock and poultry; R_i is the excretion coefficient of the livestock and poultry. The excretion coefficients of total nitrogen and total phosphorus of cattle, pigs, sheep, and poultry were recommended by the National Environmental Protection Bureau.

By adding the results of rural domestic wastes, chemical fertilizer application, and livestock breeding together, we gained the total nitrogen and total phosphorus emissions. Then, the total nitrogen and total phosphorus emissions were divided by the cultivated area of each city to obtain corresponding factors.

2.2.2. Rainfall Erosion

Rainfall is one of the dynamic factors causing soil erosion [43], and it is also the direct driving force for agricultural nonpoint source pollution. Therefore, the rainfall erosion factor [44] is commonly used to measure agricultural nonpoint source pollution caused by rainfall. This study used the soil loss measurement guidelines for production and construction projects as follows:

$$R = 0.067P^{1.627} \quad (4)$$

where R is the multi-year average rainfall erosion ($MJ \cdot mm/(hm^2 \cdot h)$); P is the average annual rainfall (mm).

2.2.3. River Network Distribution

A river network [45] is a complex network of rivers from the source to the estuary, which gathers many tributaries along the way. The river network distribution determines the regional agricultural nonpoint source pollution risk differences. To characterize the relationship between agricultural nonpoint source pollution risk and river network distance, Sivertun and Prange [46] established the weight function of pollution source to river network by calculating the distance from a single grid to the river network as follows:

$$W = \frac{0.6}{e^{0.002x} - 0.4} \quad (5)$$

where W is the river network distribution; x is the Euclidean distance (m) from each grid to the nearest river network.

2.2.4. Soil Erodibility

The soil erodibility factor is an essential indicator that represents the sensitivity of soil to erosion [47]. It reflects the impact of hydraulic power on soil's physical and chemical properties [48]. Soil types in the HRB were categorized into 20 types based on soil composition. In the USLE model, K represents the soil erodibility factor, which is determined using the following equations [49]:

$$K_{USLE} = f_{cand} \times f_{cl\text{-}si} \times f_{orgc} \times f_{hisand} \quad (6)$$

$$f_{cand} = 0.2 + 0.3 \times e^{[-0.256 \times sd \times (1 - \frac{si}{100})]} \quad (7)$$

$$f_{cl\text{-}si} = \left(\frac{si}{si + cl}\right)^{0.3} \quad (8)$$

$$f_{orgc} = 1 - \frac{0.25 \times c}{c + e^{(3.72 - 2.95 \times c)}} \tag{9}$$

$$f_{hisand} = 1 - \frac{0.7 \times (1 - \frac{sd}{100})}{\left(1 - \frac{sd}{100}\right) + e^{[-5.51 + 22.9 \times (1 - \frac{sd}{100})]}} \tag{10}$$

where the coarse gravel soil erosion factor (f_{cand}) is the percentage of gravel, the clay soil erosion factor ($f_{cl\text{-}si}$) is the percentage of silt, the soil organic matter factor (f_{orgc}) is the percentage of clay, and the high sandy soil erosion factor (f_{hisand}) is the percentage of organic carbon, all of which can be found in the Harmonized World Soil Database (HWSD) [50].

2.2.5. Slope Length

The slope length factor, related to slope and runoff catchment area, shows the impact of diverse topographical conditions on agricultural nonpoint source pollution risk [51]. It is calculated using the empirical formula of Wischmeier and Smith [52] as follows:

$$S = \begin{cases} 21.91 \sin\theta - 0.96, \ \theta \geq 10^\circ \\ 16.8 \sin\theta - 0.05, \ 5^\circ \leq \theta < 10^\circ \\ 10.8 \sin\theta + 0.03, \ \theta < 10^\circ \end{cases} \tag{11}$$

$$L = \left(\frac{\lambda}{22.13}\right)^{\alpha} \tag{12}$$

$$\alpha = \frac{\beta}{\beta + 1} \tag{13}$$

$$\beta = \left(\frac{\sin\theta}{0.0896}\right)/(3 \times \sin\theta^{0.8} + 0.56) \tag{14}$$

$$LS = L \times S \tag{15}$$

where the slope length factor L is the quantity of soil erosion normalized to a slope length of 22.13 m; θ is the angle of the slope; λ is the sum of slope length in the horizontal direction (m); α is the slope length coefficient.

2.2.6. Land Use

Land use pattern determines surface landscape structure and the nature of the underlying surface, which impacts the water cycle and material migration in the basin [53], making it an essential element in the risk of nonpoint source pollution. To simplify the calculation of risk assessment, the original land-use types were reclassified into six classes: unused land, cultivated land, forest, water area, and artificial surface. Based on Cai, Ding [54] about the relationship between land use patterns and soil erosion, the six land-use patterns were assigned as 1, 0.245, 0.1, 0, and 0.2, respectively.

2.3. Construction of Risk Assessment Model

The index system method analyzes various factors affecting agricultural nonpoint source pollution by determining the calculation method of each factor and assigning the weight value, which forms the risk assessment model. Before calculating the weight of each factor, they need to be normalized by Min-Max scaling as follows:

$$Y = \frac{X - X_{min}}{X_{max} - X_{min}} \tag{16}$$

where X and Y are the values before and after conversion; X_{max} and X_{min} are the maximum and minimum values of the samples.

The weight of different factors was estimated using the Analytic Hierarchy Process (AHP) method [55], which was proposed in the 1970s [56] as a decision-analytic method for optimizing multiple schemes and determining varying weights of each index in the building of an assessment system. The steps are as follows: (1) determine the decision-making objectives and criteria elements to establish the hierarchical structure model, (2) establish the judgment matrix based on the relative weight relationship between each index, and (3) calculate the maximum eigenvector of the judgment matrix to determine the weight of each index. In this study, we regarded the risk of nonpoint source pollution as the decision-making goal, the pollution source factors, hydrological and meteorological factors, and topographic and geological factors as the first-level indexes, the rainfall erosion, soil erodibility, slope length, river network distribution, land use, total nitrogen, and total phosphorus as the secondary indexes (Figure 2). An important feature of AHP is to identify the relative importance level of the two indexes in the form of the ratio of the importance degrees of the two indexes. For the relative weight relationship of each two indexes, we referred to the existing articles on nonpoint source pollution [14,57]. Determining the weight of each index based on AHP usually involves complicated calculations. The yaahp (Yet Another AHP) software is an AHP visual modeling and calculation platform [58,59], which provides convenient hierarchical model establishment and judgment matrix construction, saving a lot of matrix calculation steps and time. The weight of each index is then determined by using yaahp, and the weight results are shown in Table 1.

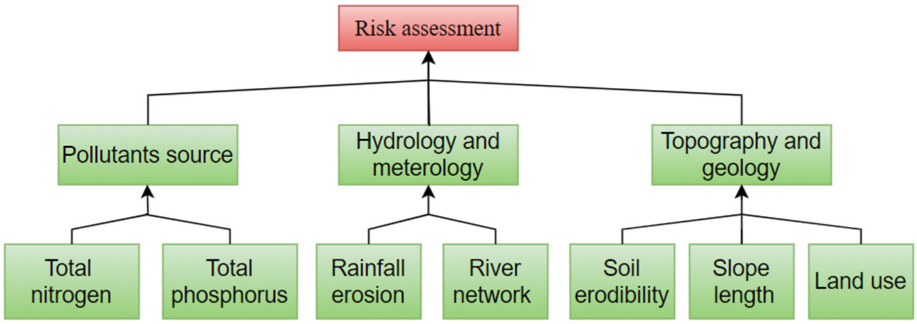

Figure 2. The AHP model structure of the risk assessment for nonpoint source pollution.

Table 1. The weight results of indexes.

First Index	Weight	Secondary Index	Weight
Pollutants source	0.3333	total nitrogen total phosphorus	0.1667 0.1667
Hydrology and meteorology	0.5000	rainfall erosion river network	0.3750 0.1250
Topography and geology	0.1667	soil erodibility slope length land use	0.0495 0.0272 0.0899

Based on the weighted results, the risk assessment model is constructed as follows:

$$\text{Risk} = 0.1667\text{TN} + 0.1667\text{TP} + 0.375\text{R} + 0.125\text{W} + 0.0495\text{K} + 0.0272\text{LS} + 0.0899\text{U} \quad (17)$$

where Risk is the total risk, TN is the total nitrogen (kg/hm^2), TP is the total phosphorus (kg/hm^2), R is rainfall erosion (MJ mm km^{-2} h^{-1} a^{-1}), W is river network distribution, K is soil erodibility, LS is slope length, U is land use.

2.4. Data Sources

The data sources we used included: (a) statistics on the total population, livestock husbandry, and fertilizer consumption from the multiple Provincial and Municipal Bureau of Statistics; (b) precipitation data of 236 stations in the HRB from the CMADS data set, which spans the period from 1 January 2014, to 31 December 2018; (c) elevation data of RTMDEM 90M in Geospatial Data Cloud; (d) soil data deriving from the HWSD created by

FAO and IIASA, with Chinese data provided at a 1:1,000,000 scale by the Institute of Soil Science, Chinese Academy of Sciences; (e) land use data from GLOBE LAND30.

2.5. Data Analysis

ArcGIS 10.7 software (ESRI, Redlands, CA, USA) was applied for the spatial analysis of each index, the construct of the risk assessment model, and the visualization. Yaahp 12.6 software (Shanxi Yuan Juece Software Technology Co., Ltd., Taiyuan, China) was used to determine the weight of each index.

3. Results

3.1. Pollution Source Analysis of TN and TP

By comparing the discrepancy in the amount of nitrogen pollution produced by different sources in the HRB, it was found that nitrogen pollution generated from fertilizer application, livestock and poultry breeding, and rural domestic wastes were 6.0308 million tons, 1.1165 million tons, and 0.1451 million tons (Table 2), accounting for 82.70%, 15.31%, and 1.99% of the total nitrogen pollution, respectively. It indicated that fertilizer application was the main source of nitrogen contamination in the HRB, followed by livestock and poultry breeding, and pollution produced by rural domestic wastes was rare. Moreover, the sources of total nitrogen emissions varied in cities (Figure 3a). It is worth noting that in cities like Linyi, Nantong, and Rizhao, in addition to the fertilizer application, more than 25% of the nitrogen emissions came from livestock and poultry breeding. On the other hand, in Zhengzhou and Zibo, compared with other cities, the nitrogen emissions generated by rural domestic wastes accounted for a larger proportion. It may be due to different cities' varied industrial layouts and governance schemes.

Table 2. Equal standard pollution load statistics (unit: 10,000 tons).

Pollution Source	TN	TP	Sum	Percentage (%)
Fertilizer pollution	603.08	136.25	739.33	81.96
Livestock and poultry breeding	111.65	35.41	147.06	16.30
Rural domestic wastes	14.51	1.17	15.68	1.74
Sum	729.24	172.83	902.07	100.00

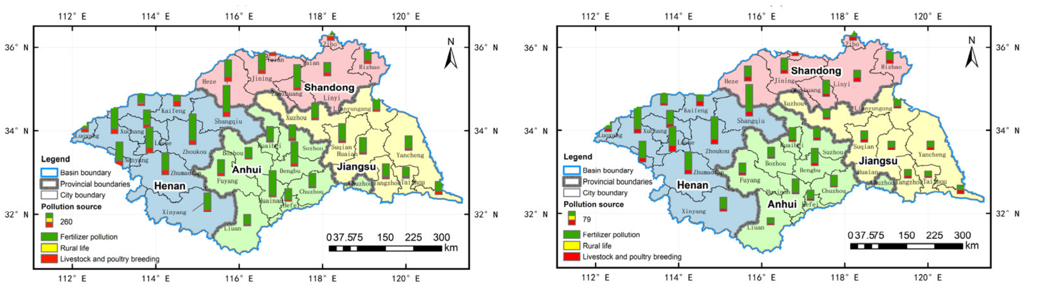

(**a**) (**b**)

Figure 3. (**a**) The distribution of TN in HRB; (**b**) the distribution of TP in HRB.

3.2. Spatial Distribution Characteristics of Each Factor

3.2.1. Total Nitrogen

In 2018, nitrogen load in 35 cities in the HRB all surpassed 180 kg/hm^2. However, it showed a decreasing trend from east to west (Figure 4a). The statistical data indicated that the average nitrogen load in the HRB was 355 kg/hm^2 and was significantly higher in Henan than in Shandong, Anhui, and Jiangsu provinces. Specifically, there was the largest nitrogen load in Pingdingshan, reaching more than 560 kg/hm^2, while most cities' nitrogen load fell to 200 to 400 kg/hm^2. On the other hand, the least nitrogen load occurred in Liu'an, with a value of 208 kg/hm^2.

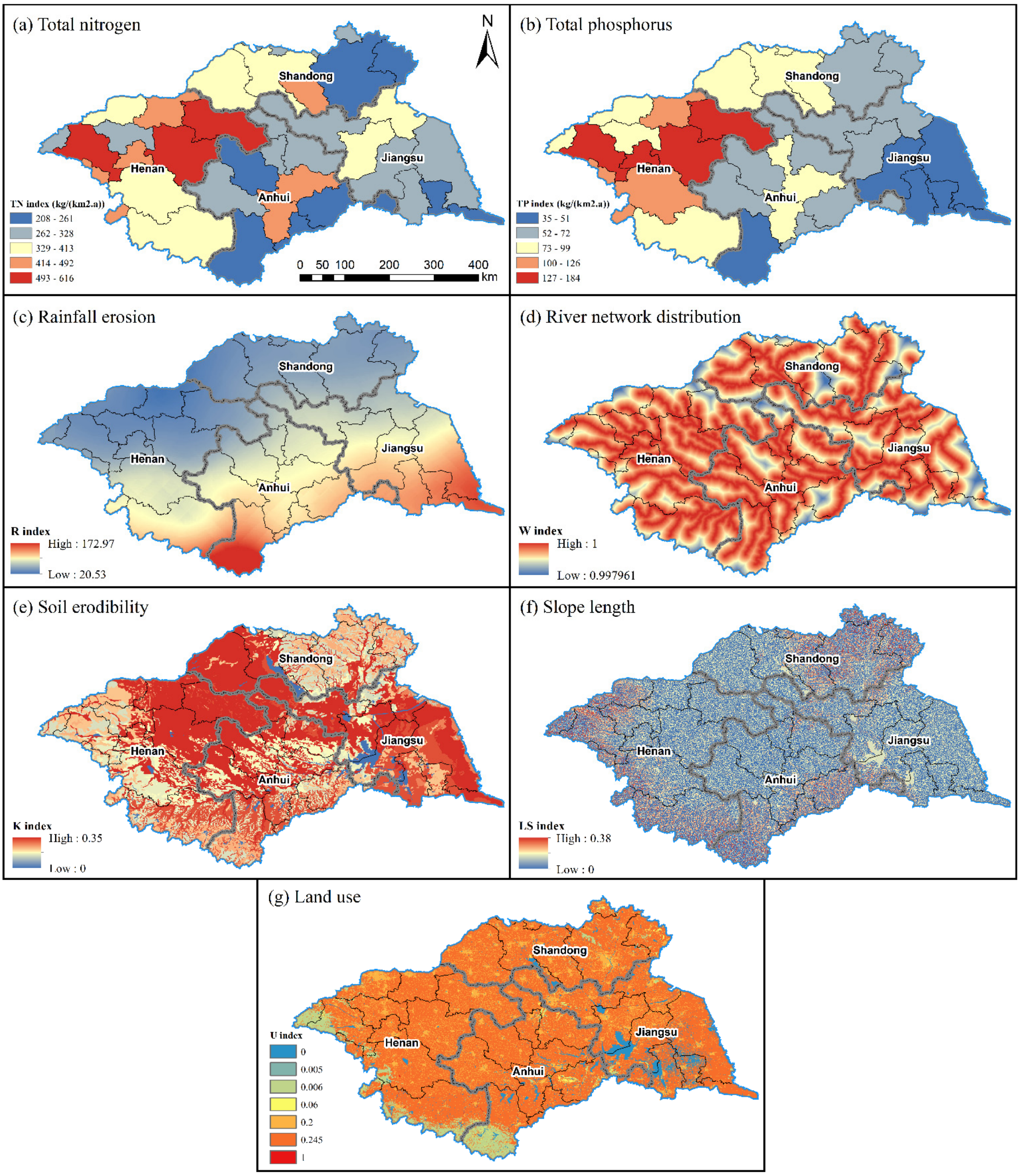

Figure 4. Spatial distribution of total nitrogen (**a**), total phosphorus (**b**), rainfall erosion (**c**), river network distribution (**d**), soil erodibility (**e**), slope length (**f**), and land use (**g**) factors in HRB.

3.2.2. Total Phosphorus

The phosphorus load gradually increased from east to west (Figure 4b). Statistics showed that the average phosphorus load in the HRB was 85 kg/hm^2. Though the amount of nitrogen and phosphorus loads differed, their distributions were similar. There was the largest phosphorus load in Pingdingshan, reaching more than 145 kg/hm^2, while the least in Tai'an, with a value of 35 kg/hm^2. Comparing the discrepancy of the phosphorus load in different cities, we found that the loading magnitude is usually higher in areas with developed planting and animal husbandry.

3.2.3. Rainfall Erosion

The regions with higher precipitation tend to have a higher risk of causing nonpoint source pollution. The distribution of the rainfall erosion factor is closely related to precipitation (Figure 4c). The near-surface of the basin is dominated by northeast wind, which is beneficial for vapor to transport to the southeast, resulting in higher precipitation in the southeast while less precipitation in the northwest. The spatial distribution of the rainfall erosion factor was characterized by decreasing from southeast to northwest. The rainfall erosion factor was higher in the south of Jiangsu and Anhui than in other regions. Liu'an in Anhui Province and Nantong in Jiangsu Province had the highest.

3.2.4. River Network Distribution

The river network distribution factor characterizes the transport distance of pollutants into the river (Figure 4d). The shorter the transport distance is, the easier the pollutants migrate into the river. The river network in the HRB is dense, so the river network distribution factor in most areas is large, indicating the high risk of pollutants entering the river.

3.2.5. Soil Erodibility

The soil erodibility factor is determined by the soil types. As shown in Figure 4e, most basin areas have high soil erodibility, and few areas have low soil erodibility, such as Nanyang, Zhumadian, and Suqian. The main soil type in the northern Huaibei Plain is yellow fluvo-aquic soil, formed from river sediments and modern yellow pan sediments. With loose soil texture and poor fertility, it is susceptible to erosion. Therefore, soil erodibility in the northern Huaibei Plain is greater than that in the western Funiu mountain (mainly cinnamon soil) and the southern Huainan mountain (mainly yellow-brown soil).

3.2.6. Slope Length

The northeast of the HRB is mountainous, and the western and southern parts are mainly hilly regions. In contrast, the central part is mainly plain (Huang-Huai-Hai alluvial plain, lacustrine plain, and marine plain). Therefore, the slope length factor in the northeast, west, and south of the basin is greater than that in the central plain area (Figure 4f). As a result, the regional pollutants with large slope length factors are easy to migrate, promoting nonpoint source pollution.

3.2.7. Land Use

More than 90% of the area in the HRB is cultivated land. The fertilizers applied for agricultural production are easily eroded by rainfall and runoff, causing severe nonpoint source pollution. In addition, with the acceleration of the urbanization process, the hardened pavement has been increasing. In contrast, forest and grassland areas have decreased, which negatively reduces the interception and purification of pollutants. As shown in Figure 4g, the land-use factor is relatively high in most areas of the HRB. Only the Tongbai Mountain and Funiu Mountain in the west and the Dabie Mountains in the south are assigned small land-use factors. The water bodies along the lower reaches of the Huaihe River, such as Hongze Lake, Gaoyou Lake, and Weishan Lake, are assigned zero values.

3.3. Spatial Distribution Characteristics of the Risk of Nonpoint Source Pollution

The weighted superposition analysis of each factor was carried out to obtain a comprehensive evaluation of the nonpoint source pollution risk (Figure 5). For the calculation results, the natural discontinuity method was used for classification and display, which sets the discontinuous point at the position where the difference in the data value is the largest. With this method, the similarity within a group can be maximized; meanwhile, the difference between groups can be maximized; hence it is reasonable to classify the risk levels. After classification, the HRB was divided into five categories, and the area proportion of each risk level area is shown in Table 3.

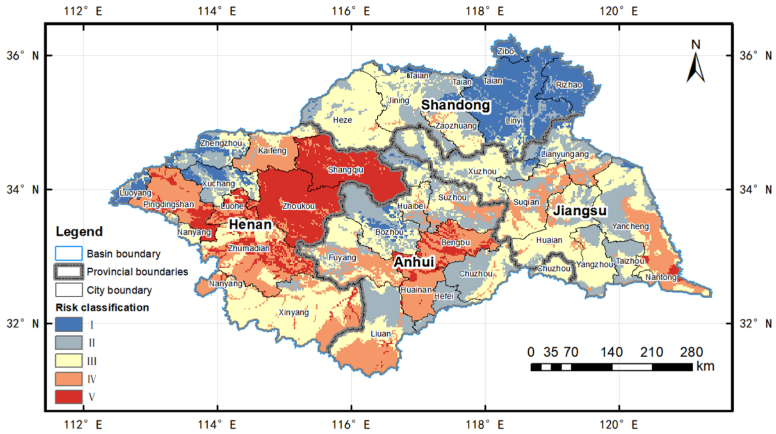

Figure 5. Spatial distribution of nonpoint source pollution risk.

Table 3. Risk level statistics.

Risk Level	I	II	III	IV	V
Area (km^2)	30,760	61,446	91,995	56,494	33,962
Percentage (%)	11.20	22.37	33.49	20.57	12.37

The results showed that more than 60% of the areas in the HRB were at the median, relatively high, or high risk of nonpoint source pollution, and the high-risk account for 12.37%, occupying an area of 33,962 km^2. Regions with relatively high risk were mainly concentrated in Henan and Anhui provinces, of which Shangqiu and Zhoukou cities were entirely in the high-risk group. In addition to the concentrated distribution areas in Henan and Anhui provinces, the areas with median risk were distributed along the mainstream of the Huaihe River. While the proportion of low-risk regions was 11.20%, covering an area of 30,760 km^2, mainly distributed in Shandong Province. Among the regions in Shandong Province, cities like Zibo, Rizhao, and Linyi were all at low risk.

For high-risk areas, the emissions of nitrogen and phosphorus pollutants were large, the rainfall and soil erodibility factors were high, and the terrain was steep. In contrast, the interception and purification effect of land use patterns on pollutants was small, and the distance from the emission point to the nearest water body was short. Therefore, under the combined effects of source factors, hydrometeorological factors, and topographic and geological factors, the flux of pollutants into rivers in high-risk areas was relatively high. Therefore, the management and control of rural domestic wastes, livestock and poultry excrement, and fertilizer application should be strengthened. Effective measures include enhancing public awareness of environmental protection, advocating clean producing, and improving farming methods. Furthermore, from the perspective of weakening the migration process of pollutants, the pollutants in the runoff process could be intercepted and purified by increasing vegetation coverage, establishing buffer zones, and reducing hardened pavements, which reduce the discharge of pollutants into water bodies.

The amount of phosphorus pollution was not as much as nitrogen pollutants (Figure 3b). By analyzing the discrepancy in the amount of phosphorus pollution produced by different sources in the HRB, it was found that the phosphorus emissions generated from fertilizer application, livestock and poultry breeding, and rural domestic wastes were 1.3625 million tons, 0.3541 million tons and 0.0117 million tons, accounting for 78.83%, 20.49% and 0.68% of total phosphorus respectively. The application of phosphate fertilizer and compound fertilizer was the main source of phosphorus contamination in the HRB, while pollution from rural domestic wastes was so little that it could be almost neglected. Besides, in some cities, livestock and poultry breeding also led to the generation of a lot of phosphorus. For example, more than 30% of phosphorus pollution was produced by livestock and poultry breeding in Nantong, Linyi, Yancheng, and Rizhao.

The analysis of the total emission sources of nitrogen and phosphorus (Table 2) showed: fertilizer application (81.96%) > livestock and poultry breeding (16.3%) > rural domestic wastes (1.74%). Therefore, the watershed environmental governance should focus on farmland planting and livestock and poultry breeding. Especially in fertilizer applications for farmland planting, it is easy to produce nitrogen and phosphorus contaminants because the compounds put into farmland enter the water body through volatilization and loss. In addition, each city's pollution source difference has a certain relationship with its population, crop planting area, and industrial structure. Therefore, by understanding the composition of pollution sources in different cities, it is convenient to trace and remediate different pollutants from the source to achieve efficient water environment management.

4. Discussion

4.1. Validation of the Risk Assessment Results

To verify the accuracy of the risk assessment results of nonpoint source pollution, we obtained the observed water quality class data of 160 monitoring sections in the HRB from the China National Environmental Monitoring Centre, with their spatial distribution shown in Figure 6a. The observed water quality data showed that the water quality of the main rivers in the HRB fell in the clean category. The monitoring sections of Class IV and ClassV water quality are mainly distributed in Rizhao in Shandong and Shangqiu and Zhoukou in Henan. The water quality in the northern cities of Shandong and the western cities of Henan is relatively good, most of which are of type I and II. To compare differences between the risk assessment results and the measured water quality more intuitively, we extracted the risk class value at the location of the monitoring section (Figure 6b) and subtracted the water quality from the risk class value for deviation analysis.

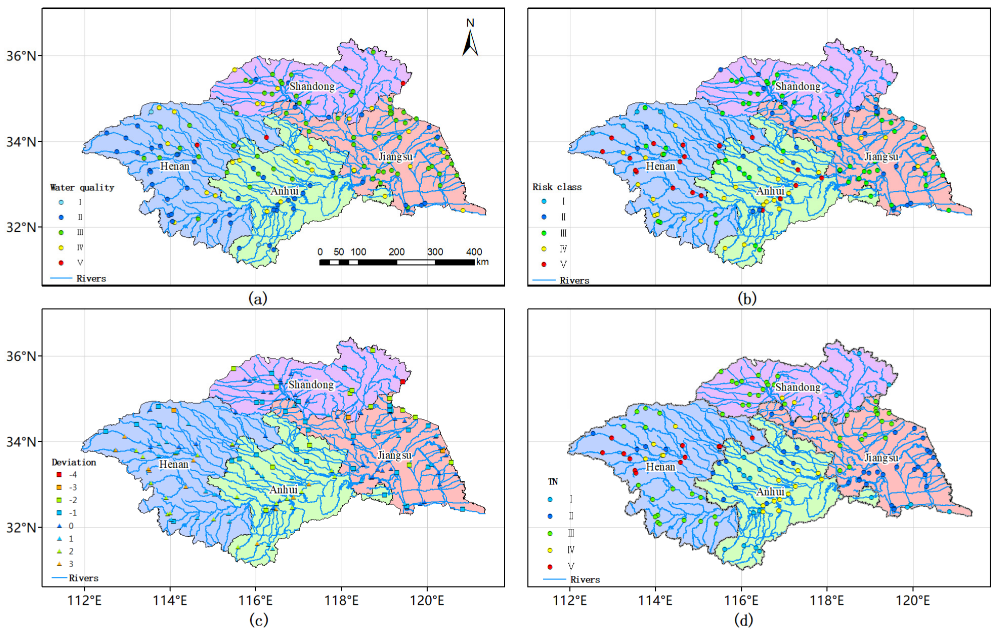

Figure 6. The water quality (**a**), risk class (**b**), the deviation between water quality and risk class (**c**), and TN distribution (**d**) of monitoring sections.

After deviation analysis and statistics (Figure 6c), among the 160 monitoring sections, there are 48 sections with a deviation value of 0, accounting for 30.0%, 51 sections with a deviation value less than 0, accounting for 31.9%, and 61 sections with a deviation value greater than 0, accounting for 38.1%. While 0 represents proper evaluation, the section with a deviation value greater than 0 is overestimated, or vice versa. The section with the maximum deviation is approximately located east of Shandong. Sections with a deviation value of 0 and ±1 are roughly distributed throughout the basin.

Overall, most deviation values of the monitoring sections in Jiangsu and Shandong are 0. The deviation values in Anhui and Henan provinces are relatively evenly distributed from −1 to 3. The sections with a deviation value of 0 or ±1 accounted for 70.6%, indicating that the risk assessment results are accurate and the overall deviation is relatively small. It should be noted that the risk assessment results are only for nonpoint source pollution, and only the typical nonpoint source pollutants (i.e., total nitrogen and total phosphorus) were considered. Therefore, while the water quality of the monitoring section is the result of point source and nonpoint source pollution, inevitably, there are some deviations between the evaluation results and the measured water quality data.

The overestimated sections are mainly distributed in Henan and Anhui, where large amounts of nitrogen (Figure 6d) and phosphorus loads are investigated. To quickly identify the controlling areas of NPS pollution in HRB, some local policies that mitigate water pollution were not considered. This simplification led to the overestimation of TP and TP, especially for regions that face severe water environment issues and have plenty of room for improvements, such as Henan and Anhui. In the past few years, Henan has strengthened the supervision of the agricultural and rural environment and continued to promote the rectification of domestic sewage, livestock and poultry breeding, and agricultural fertilizer application. The river chief system [60] was established in HRB in 2017. Studies in Chaohu lake [61] and Foshan [62] have proved that the river chief system is effective in managing water pollution. Measures such as increasing sewage treatment plants, strengthening the construction of cleaning infrastructure, and standardizing the application of fertilizers can reduce the pollutants output by human activities. However, policy performance is difficult to quantify in our risk assessment model, resulting in the overestimation of TN and TP loads.

The underestimated sections are mainly distributed in estuaries. The estuaries not only receive sewage from local and adjacent areas but are also affected by accidental spills at sea. A study in Newark Bay, New Jersey [63] indicated that combined sewer overflows in the urban system have been an important point source pollution and have a significant impact on ecology [64]. Accidental spills of oils and chemicals at sea also damage the aquatic environment [65,66]. The effects of combined sewer overflows and accidental spills are not included in our model. The Bulletin of Marine Ecology and Environment Status of China in 2021 [67] reported that the water quality of estuaries in Shandong Province is mildly polluted. The main indicators exceeding the standard are the permanganate index, chemical oxygen demand (COD), and five-day biochemical oxygen demand (BOD_5). Our risk assessment model of nonpoint source pollution only considers TN and TP loads, while organic pollutants are excluded. Therefore, the risk class in estuaries is lower than the measured water quality class.

4.2. Limitations

4.2.1. Limitations of Data and Methods

We acknowledge that there are some limitations to the data and methods. Due to the data availability, the estimation of nitrogen and phosphorus loads was based on the statistics from the Provincial and Municipal Bureau of Statistics in 2018 rather than the long-term average value, which may make the data lack a strong representation. Besides, in terms of the analytic hierarchy process method, we determined the relative weight relationship between each indicator by referring to the previous studies. Further study should be improved by seeking expert opinions and conducting a field investigation to determine each factor's weight. Despite these limitations, our results are accurate, and our methods would be useful for similar applications.

4.2.2. Pollution Source Indicators

For the initial goal of constructing a risk assessment model to identify the hotspots of nonpoint source pollution quickly, some simplifications were made. For example, although we selected nitrogen and phosphorus emissions as pollution indicators, other sources, such as ammonia nitrogen and chemical oxygen demand, were not included. In addition, due to limited statistics, we did not distinguish the discrepancy in sewage discharge mode between rural and urban and used the same emission coefficient for calculation. In future studies, these issues should be considered. However, the result of our study on pollution sources was considerable and consistent with relevant studies on the HRB.

5. Conclusions

In this study, we applied the method of index system to build a risk assessment model of nonpoint source pollution in the HRB. We studied the distribution characteristics of seven risk factors that affected nonpoint source pollution and identified the potential risk controlling area based on our model.

The primary source of total nitrogen and phosphorus loads is fertilizer application (81.96%), followed by livestock and poultry breeding (16.3%) and rural domestic wastes (1.74%). The distributions of TN and TP pollution are similar, and the amount of emission reaches the largest in the central and eastern Henan Province. 66.43% of the HRB is at medium, relatively high, and high risk of nonpoint source pollution. Specifically, 12.37% of the basin is at high risk, covering an area of 33,962 km^2, and 11.20% of the area is at low risk, covering an area of 30,760 km^2. The medium-to-high-risk areas are mainly concentrated in the Henan and Anhui provinces. In contrast, the medium-risk regions are mainly distributed along the mainstream of the Huaihe River. These areas are more likely to lose nutrients such as nitrogen and phosphorus and should be considered critical for preventing nonpoint source pollution.

To prevent and control the nonpoint source pollution in HRB, measures should be taken to strengthen the management of fertilizer application, livestock and poultry, and rural domestic wastes, as well as weaken the migration process of pollutants by measures such as increasing vegetation coverage and establishing buffer zones, all of which are expected to reduce the pollution loadings into water bodies.

Author Contributions: Conceptualization, H.Z. and X.C.; methodology, H.Z.; validation, H.Z.; formal analysis, J.Z. and Y.Z.; investigation, J.Z.; resources, Y.Z.; data curation, Y.Z.; writing—original draft preparation, H.Z., J.Z. and Y.Z.; writing—review and editing, X.C. and L.L.; visualization, J.Z.; supervision, X.C.; project administration, X.C.; funding acquisition, X.C. All authors have read and agreed to the published version of the manuscript.

Funding: This work is supported by the Natural Science Foundation of Guangdong Province, China (Grant No. 2022A1515010676) and the Innovation and Entrepreneurship Training Program for College Students of Sun Yat-sen University.

Data Availability Statement: The data supporting our work have been listed in Section 2.4 of the main text and are openly available. Any requests for the raw data can be made to the corresponding author(s).

Acknowledgments: We are grateful for the input and evaluation data from multiple Provincial and Municipal Bureau of Statistics, the China Meteorological Assimilation Driving Datasets for the SWAT model (CMADS), the Food and Agriculture Organization (FAO), the International Institute for Applied Systems Analysis (IIASA), and the Institute of Soil Science, Chinese Academy of Sciences (ISSAS).

Conflicts of Interest: The funders had no role in the design of the study; in the collection, analyses, or interpretation of data; in the writing of the manuscript; or in the decision to publish the results.

References

1. Greve, P.; Kahil, T.; Mochizuki, J.; Schinko, T.; Satoh, Y.; Burek, P.; Fischer, G.; Tramberend, S.; Burtscher, R.; Langan, S.; et al. Global assessment of water challenges under uncertainty in water scarcity projections. *Nat. Sustain.* **2018**, *1*, 486–494. [CrossRef]
2. Boretti, A.; Rosa, L. Reassessing the projections of the world water development report. *NPJ Clean Water* **2019**, *2*, 15. [CrossRef]
3. Leal Filho, W.; Totin, E.; Franke, J.A.; Andrew, S.M.; Abubakar, I.R.; Azadi, H.; Nunn, P.D.; Ouweneel, B.; Williams, P.A.; Simpson, N.P.; et al. Understanding responses to climate-related water scarcity in Africa. *Sci. Total Environ.* **2022**, *806*, 150420. [CrossRef] [PubMed]

4. Abedin, M.A.; Collins, A.E.; Habiba, U.; Shaw, R. Climate Change, Water Scarcity, and Health Adaptation in Southwestern Coastal Bangladesh. *Int. J. Disaster Risk Sci.* **2019**, *10*, 28–42. [CrossRef]
5. Ma, T.; Sun, S.; Fu, G.; Hall, J.W.; Ni, Y.; He, L.; Yi, J.; Zhao, N.; Du, Y.; Pei, T.; et al. Pollution exacerbates China's water scarcity and its regional inequality. *Nat. Commun.* **2020**, *11*, 650. [CrossRef]
6. van Vliet, M.T.; Jones, E.R.; Flörke, M.; Franssen, W.H.; Hanasaki, N.; Wada, Y.; Yearsley, J.R. Global water scarcity including surface water quality and expansions of clean water technologies. *Environ. Res. Lett.* **2021**, *16*, 024020. [CrossRef]
7. Iqbal, M.M.; Hussain, S.; Cheema, E.M.J.; Lee, J.; Waqas, M.; Aslam, M. Seasonal effect of agricultural pollutants on coastline environment a case study of the southern estuarine water ecosystem of the boseong county Korea. *Pak. J. Agric. Res.* **2022**, *59*, 117–124. [CrossRef]
8. Iqbal, M.M.; Li, L.; Hussain, S.; Lee, J.L.; Mumtaz, F.; Elbeltagi, A.; Waqas, M.S.; Dilawar, A. Analysis of Seasonal Variations in Surface Water Quality over Wet and Dry Regions. *Water* **2022**, *14*, 1058. [CrossRef]
9. Iqbal, M.M.; Shoaib, M.; Farid, H.U.; Lee, J.L. Assessment of water quality profile using numerical modeling approach in major climate classes of Asia. *Int. J. Environ. Res. Public Health* **2018**, *15*, 2258. [CrossRef]
10. Wang, J.; Zhao, J.; Lei, X.; Wang, H. New approach for point pollution source identification in rivers based on the backward probability method. *Environ. Pollut.* **2018**, *241*, 759–774. [CrossRef]
11. Kaushal, S.S.; Groffman, P.M.; Band, L.E.; Elliott, E.M.; Shields, C.A.; Kendall, C. Tracking Nonpoint Source Nitrogen Pollution in Human-Impacted Watersheds. *Environ. Sci. Technol.* **2011**, *45*, 8225–8232. [CrossRef] [PubMed]
12. Jia, Z.; Tang, S.; Luo, W.; Hai, Y. Water quality improvement through five constructed serial wetland cells and its implications on nonpoint-source pollution control. *Hydrol. Sci. J.* **2016**, *61*, 2946–2956. [CrossRef]
13. Dowd, B.M.; Press, D.; Huertos, M.L. Agricultural nonpoint source water pollution policy: The case of California's Central Coast. *Agric. Ecosyst. Environ.* **2008**, *128*, 151–161. [CrossRef]
14. Zou, L.; Liu, Y.; Wang, Y.; Hu, X. Assessment and analysis of agricultural non-point source pollution loads in China: 1978–2017. *J. Environ. Manag.* **2020**, *263*, 110400. [CrossRef] [PubMed]
15. Han, J.; Xin, Z.; Han, F.; Xu, B.; Wang, L.; Zhang, C.; Zheng, Y. Source contribution analysis of nutrient pollution in a P-rich watershed: Implications for integrated water quality management. *Environ. Pollut.* **2021**, *279*, 116885. [CrossRef]
16. Boers, P.C.M. Nutrient emissions from agriculture in the Netherlands, causes and remedies. *Water Sci. Technol.* **1996**, *33*, 183–189. [CrossRef]
17. Grizzetti, B.; Bouraoui, F.; Granlund, K.; Rekolainen, S.; Bidoglio, G. Modelling diffuse emission and retention of nutrients in the Vantaanjoki watershed (Finland) using the SWAT model. *Ecol. Model.* **2003**, *169*, 25–38. [CrossRef]
18. Ongley, E.D.; Zhang, X.L.; Yu, T. Current status of agricultural and rural non-point source Pollution assessment in China. *Environ. Pollut.* **2010**, *158*, 1159–1168. [CrossRef]
19. Chen, D.; Huang, H.; Hu, M.; Dahlgren, R.A. Influence of lag effect, soil release, and climate change on watershed anthropogenic nitrogen inputs and riverine export dynamics. *Environ. Sci. Technol.* **2014**, *48*, 5683–5690. [CrossRef]
20. Douglas-Mankin, K.R.; Srinivasan, R.; Arnold, J.G. Soil and Water Assessment Tool (SWAT) Model: Current Developments and Applications. *Trans. ASABE* **2010**, *53*, 1423–1431. [CrossRef]
21. Li, M.; Guo, Q. SWAT model simulation of non-point source pollution in the Miyun Reservoir Watershed. In Proceedings of the 7th Annual International Conference on Geo-Spatial Knowledge and Intelligence, Guangzhou, China, 20–21 December 2019; p. 012075.
22. Bingner, R.L.; Theurer, F.D.; Yuan, Y. *AnnAGNPS Technical Processes*; USDA-ARS. National Sedimentation Laboratory: Oxford, UK, 2003.
23. Zhang, T.; Yang, Y.; Ni, J.; Xie, D. Best management practices for agricultural non-point source pollution in a small watershed based on the Ann AGNPS model. *Soil Use Manag.* **2020**, *36*, 45–57. [CrossRef]
24. Li, Z.; Liu, H.-Y.; Li, Y. Review on HSPF model for simulation of hydrology and water quality processes. *Huan Jing Ke Xue* **2012**, *33*, 2217–2223. [PubMed]
25. Bai, X.; Shen, W.; Wang, P.; Chen, X.; He, Y. Response of non-point source pollution loads to land use change under different precipitation scenarios from a future perspective. *Water Resour. Manag.* **2020**, *34*, 3987–4002. [CrossRef]
26. Shen, Z.; Liao, Q.; Hong, Q.; Gong, Y. An overview of research on agricultural non-point source pollution modelling in China. *Sep. Purif. Technol.* **2012**, *84*, 104–111. [CrossRef]
27. Wang, M.; Chen, L.; Wu, L.; Zhang, L.; Xie, H.; Shen, Z. Review of Nonpoint Source Pollution Models: Current Status and Future Direction. *Water* **2022**, *14*, 3217. [CrossRef]
28. Omernik, J.M. *The Influence of Land Use on Stream Nutrient Levels*; US Environmental Protection Agency, Office of Research and Development: Washington, DC, USA, 1976.
29. Johnes, P.J. Evaluation and management of the impact of land use change on the nitrogen and phosphorus load delivered to surface waters: The export coefficient modelling approach. *J. Hydrol.* **1996**, *183*, 323–349. [CrossRef]
30. Cheng, X.; Chen, L.; Sun, R.; Jing, Y. An improved export coefficient model to estimate non-point source phosphorus pollution risks under complex precipitation and terrain conditions. *Environ. Sci. Pollut. Res.* **2018**, *25*, 20946–20955. [CrossRef]
31. Ding, X.; Shen, Z.; Hong, Q.; Yang, Z.; Wu, X.; Liu, R. Development and test of the export coefficient model in the upper reach of the Yangtze River. *J. Hydrol.* **2010**, *383*, 233–244. [CrossRef]

32. Hua, L.; Li, W.; Zhai, L.; Yen, H.; Lei, Q.; Liu, H.; Ren, T.; Xia, Y.; Zhang, F.; Fan, X. An innovative approach to identifying agricultural pollution sources and loads by using nutrient export coefficients in watershed modeling. *J. Hydrol.* **2019**, *571*, 322–331. [CrossRef]
33. Bhattacharjee, J.; Marttila, H.; Launiainen, S.; Lepisto, A.; Klove, B. Combined use of satellite image analysis, land-use statistics, and land-use-specific export coefficients to predict nutrients in drained peatland catchment. *Sci. Total Environ.* **2021**, *779*, 146419. [CrossRef]
34. Guo, H.Y.; Wang, X.R.; Zhu, J.G. Quantification and Index of Non-Point Source Pollution in Taihu Lake Region with GIS. *Environ. Geochem. Health* **2004**, *26*, 147–156. [CrossRef] [PubMed]
35. Guo, H.; Zhu, J.; Wang, X.; Wu, Z.; Zhang, Z. Case study on nitrogen and phosphorus emissions from paddy field in Taihu region. *Environ. Geochem. Health* **2004**, *26*, 209–219. [CrossRef] [PubMed]
36. Lemunyon, J.L.; Gilbert, R.G. The Concept and Need for a Phosphorus Assessment Tool. *J. Prod. Agric.* **1993**, *6*, 483–486. [CrossRef]
37. Ministry of Ecology and Environment of China. China Ecological Environment Status Bulletin 2020 (Excerpt). *Environ. Prot.* **2021**, *49*, 47–68. [CrossRef]
38. Li, X. Pay close attention to the prevention and control of agricultural non-point source pollution, promote the development of ecological economy in the Huaihe River Basin: Investigation report on the control of non-point source pollution in the Huaihe River Basin. *China Econ. Trade Her.* **2019**, 48–52.
39. Song, D.; Zuo, Q.; Liu, B.; Zou, G.; Liu, D. Estimation of spatio-temporal variability and health risks of nitrogen emissions from agricultural non-point source pollution: A case study of the Huaihe River Basin, China. *J. Agro-Environ. Sci.* **2018**, *37*, 1219–1231.
40. Zhang, H.; Huang, G.H. Assessment of non-point source pollution using a spatial multicriteria analysis approach. *Ecol. Model.* **2011**, *222*, 313–321. [CrossRef]
41. Wang, H.; Liu, Z.; Zhu, J.; Chen, D.; Qin, F. Spatio-Temporal Extraction of Surface Waterbody and Its Response of Extreme Climate along the Upper Huaihe River. *Sustainability* **2022**, *14*, 3223. [CrossRef]
42. National Water Resources Comprehensive Planning Group. *Supplementary Rules for Surface Water Quality Assessment and Pollutant Emission Survey and Estimation of National Water Resources Comprehensive Planning*; Water Conservancy and Hydropower Planning and Design Institute, Ministry of Water Resources: Beijing, China, 2003.
43. Teng, H.-F.; Hu, J.; Zhou, Y.; Zhou, L.-Q.; Shi, Z. Modelling and mapping soil erosion potential in China. *J. Integr. Agric.* **2019**, *18*, 251–264. [CrossRef]
44. Yin, S.; Nearing, M.A.; Borrelli, P.; Xue, X. Rainfall Erosivity: An Overview of Methodologies and Applications. *Vadose Zone J.* **2017**, *16*, 1–16. [CrossRef]
45. Peucker, T.K.; Douglas, D.H. Detection of Surface-Specific Points by Local Parallel Processing of Discrete Terrain Elevation Data. *Comput. Graph. Image Process.* **1975**, *4*, 375–387. [CrossRef]
46. Sivertun, Å.; Prange, L. Non-point source critical area analysis in the Gisselö watershed using GIS. *Environ. Model. Softw.* **2003**, *18*, 887–898. [CrossRef]
47. Huang, X.; Lin, L.; Ding, S.; Tian, Z.; Zhu, X.; Wu, K.; Zhao, Y. Characteristics of Soil Erodibility K Value and Its Influencing Factors in the Changyan Watershed, Southwest Hubei, China. *Land* **2022**, *11*, 134. [CrossRef]
48. Krasa, J.; Dostal, T.; Jachymova, B.; Bauer, M.; Devaty, J. Soil erosion as a source of sediment and phosphorus in rivers and reservoirs—Watershed analyses using WaTEM/SEDEM. *Environ. Res.* **2019**, *171*, 470–483. [CrossRef]
49. Williams, J.R.; Renard, K.G.; Dyke, P.T. EPIC: A new method for assessing erosion's effect on soil productivity. *J. Soil Water Conserv.* **1983**, *38*, 381–383.
50. FAO/IISA/ISRIC/ISS-CAS/JRC. *Harmonized World Soil Database, Version 1.2*; FAO and IIASA: Laxenberg, Austria, 2012.
51. Konstantinos, K.; Vassilios, P.; al Sayah, M.J.; Simone, S.; Maurizio, R. A USLE-based model with modified LS-factor combined with sediment delivery module for Alpine basins. *Catena* **2021**, *207*, 105655.
52. Wischmeier, W.H.; Smith, D.D. *Predicting Rainfall Erosion Losses: A Guide to Conservation Planning*; Science and Education Administration, United States Department of Agriculture: Washington, DC, USA, 1978.
53. Zhang, J.; Li, S.; Dong, R.; Jiang, C.; Ni, M. Influences of land use metrics at multi-spatial scales on seasonal water quality: A case study of river systems in the Three Gorges Reservoir Area, China. *J. Clean. Prod.* **2019**, *206*, 76–85. [CrossRef]
54. Cai, C.; Ding, S.; Shi, Z.; Huang, L.; Zhang, G. Study of Applying USLE and Geographical Information System IDRISI to Predict Soil Erosion in Small Watershed. *J. Soil Water Conserv.* **2000**, *14*, 19–24. [CrossRef]
55. Saaty, R.W. The analytic hierarchy process—What it is and how it is used. *Math. Model.* **1987**, *9*, 161–176. [CrossRef]
56. Dodd, F.J.; Donegan, H.A.; McMaster, T.B.M. A statistical approach to consistency in AHP. *Math. Comput. Model.* **1993**, *18*, 19–22. [CrossRef]
57. Yang, J.; Feng, A.-P.; Wang, X.; Li, X.; Wang, C.; Tian, Z. An identification method of potential risk for agricultural non-point source pollution in the Haihe River Basin. *China Environ. Sci.* **2021**, *41*, 4782–4791. [CrossRef]
58. Liu, Y. Construction of the Professional Quality Evaluation System of Environmental Impact Assessment Engineers Based on Yaahp Software. *E3S Web Conf.* **2021**, *259*, 05002.
59. Ming, C.; Changxin, X.; Hongquan, C. Development of Evaluation System of Coastline Resource in Dafeng. *Pol. Marit. Res.* **2017**, *24*, 181–187. [CrossRef]

60. Zhang, Z.; Xiong, C.; Yang, Y.; Liang, C.; Jiang, S. What Makes the River Chief System in China Viable? Examples from the Huaihe River Basin. *Sustainability* **2022**, *14*, 6329. [CrossRef]
61. Xu, X.; Wu, F.; Zhang, L.; Gao, X. Assessing the Effect of the Chinese River Chief Policy for Water Pollution Control under Uncertainty-Using Chaohu Lake as a Case. *Int. J. Environ. Res. Public Health* **2020**, *17*, 3103. [CrossRef]
62. Liu, H.; Chen, Y.D.; Liu, T.; Lin, L. The River Chief System and River Pollution Control in China: A Case Study of Foshan. *Water* **2019**, *11*, 1606. [CrossRef]
63. Crawford, D.W.; Bonnevie, N.L.; Wenning, R.J. Sources of Pollution and Sediment Contamination in Newark Bay, New Jersey. *Ecotoxicol. Environ. Saf.* **1995**, *30*, 85–100. [CrossRef]
64. Nie, J.; Feng, H.; Witherell, B.B.; Alebus, M.; Mahajan, M.D.; Zhang, W.; Yu, L. Causes, Assessment, and Treatment of Nutrient (N and P) Pollution in Rivers, Estuaries, and Coastal Waters. *Curr. Pollut. Rep.* **2018**, *4*, 154–161. [CrossRef]
65. Kirby, M.F.; Law, R.J. Accidental spills at sea—Risk, impact, mitigation and the need for co-ordinated post-incident monitoring. *Mar. Pollut. Bull.* **2010**, *60*, 797–803. [CrossRef]
66. Short, J.W. Advances in Understanding the Fate and Effects of Oil from Accidental Spills in the United States Beginning with the Exxon Valdez. *Arch. Environ. Contam. Toxicol.* **2017**, *73*, 5–11. [CrossRef]
67. Ministry of Ecology and Environment of China. *Bulletin of Marine Ecology and Environment Status of China in 2021*; Ministry of Ecology and Environment of China: Beijing, China, 2022.